

(3/29/2007)

Observational Constraints on Dark Energy and Cosmological Curvature

Yun Wang¹, and Priya Mukherjee²

¹ Homer L. Dodge Department of Physics & Astronomy, Univ. of Oklahoma,
440 W Brooks St., Norman, OK 73019; email: wang@nhn.ou.edu and

² Department of Physics & Astronomy, Univ. of Sussex, Falmer,
Brighton, BN1 9QH, UK; email: p.mukherjee@sussex.ac.uk

Current observational bounds on dark energy depend on our assumptions about the curvature of the universe. We present a consistent and simple framework for incorporating constraints from Cosmic Microwave Background (CMB) anisotropy data, into an analysis with other cosmological data, when constraining dark energy without assuming a flat universe.

We show that there are two CMB shift parameters, $R = \frac{m}{H_0} \frac{r}{r_s}$ (the scaled distance to recombination) and $l_a = r_s(z_{\text{CMB}})$ (the angular scale of the sound horizon at recombination); they have measured values that are nearly uncorrelated with each other. We demonstrate that both R and l_a (together with bh^2) must be used to describe the complex degeneracies amongst the cosmological parameters that determine the CMB angular power spectrum. Using both R and l_a helps break the degeneracy between the dark energy density function $X(z) = x(z) - x(0)$ and cosmological curvature. Allowing non-zero cosmological curvature, the three-year WMAP data give $R = 1.71 \pm 0.03$, $l_a = 302.5 \pm 1.2$, and $bh^2 = 0.02173 \pm 0.00082$, independent of the dark energy model. The corresponding bounds for a flat universe are $R = 1.70 \pm 0.03$, $l_a = 302.2 \pm 1.2$, and $bh^2 = 0.022 \pm 0.00082$. We give the covariance matrix of (R, l_a, bh^2) from the three-year WMAP data.

Assuming the HST prior of $H_0 = 72 \pm 8$ (km/s) Mpc⁻¹, using 182 SNe Ia (from the HST/GOODS program, the first year Supernova Legacy Survey, and nearby SN Ia surveys), CMB data, and SDSS measurement of the baryon acoustic oscillation scale, we find that dark energy density is consistent with a constant in cosmological time, with marginal deviations from a cosmological constant that may reflect current systematic uncertainties or true evolution in dark energy. A flat universe is allowed by current data at the 68% confidence level. The bounds on cosmological curvature are less stringent if dark energy density is allowed to be a free function of cosmological time, and are also dependent on the assumption about the early time property of dark energy. Significant improvement in dark energy and cosmological curvature constraints is expected as a result of future dark energy and CMB experiments.

PACS numbers: 98.80.Es, 98.80.-k, 98.80.Jk

Keywords: Cosmology

I. INTRODUCTION

The unknown cause for the observed cosmological acceleration [1, 2], dubbed "dark energy", remains the most compelling mystery in cosmology today. Dark energy could be an unknown energy component [3, 4, 5, 6, 7, 8], or a modification of general relativity [9, 10, 11, 12, 13, 14]. [15] and [16] contain reviews of many models. Dark energy modelbuilding is a very active research area. For recent dark energy models, see for example, [17, 18, 19, 20, 21, 22, 23]. Current observational data continue to be consistent with dark energy being a cosmological constant, but the evidence for a cosmological constant is not conclusive and more exotic possibilities are still allowed (see, for example, [24, 25, 26, 27, 28, 29, 30, 31, 32, 33, 34, 35, 36, 37, 38, 39, 40, 41, 42, 43, 44]).

While the universe is completely consistent with being flat under a CDM hypothesis, it is important to note that the observational bounds on dark energy and the curvature of the universe are closely related. Cosmological microwave background (CMB) anisotropy data provide the most stringent constraints on cosmological curvature κ . Assuming that dark energy is a cosmological constant, the

three-year WMAP data give $\kappa = 0.15 \pm 0.11$, and this improves dramatically to $\kappa = 0.005 \pm 0.006$ with the addition of galaxy survey data from the SDSS [45] (2dF data [46] also give a similar improvement) [55]. The effect of allowing non-zero curvature on constraining some dark energy models has been studied by [47, 48, 49, 50, 51].

In this paper, we present a consistent and simple framework for incorporating constraints from the CMB data into an analysis with other cosmological data in constraining dark energy without assuming a flat universe. Using this framework, we derive constraints on dark energy and cosmological curvature using CMB, type Ia supernova (SN Ia) and galaxy survey data.

We describe our method in Sec. 2, present our results in Sec. 3, and conclude in Sec. 4.

II. METHOD

A. The Basic Approach

The comoving distance from the observer to redshift z is given by

$$r(z) = \frac{cH_0}{Z} \int_0^z \frac{dz'}{E(z')}; \quad E(z) = H(z) = H_0 \frac{1}{a}; \quad (1)$$

where $k = H_0^2$ with k denoting the curvature constant, and $\sinh(x) = \sin(x)$, x , $\sinh(x)$ for $k < 0$, $k = 0$, and $k > 0$ respectively, and

$$E(z) = \frac{m}{m} (1+z)^3 + \frac{rad}{rad} (1+z)^4 + \frac{k}{k} (1+z)^2 + \frac{x}{x} X(z)^{1/2}; \quad (2)$$

with $x = 1 - \frac{m}{m} - \frac{rad}{rad} - \frac{k}{k}$, and the dark energy density function $X(z) = x(0)$.

CMB data give us the comoving distance to the recombination surface $r(z_{\text{CMB}})$ with $z_{\text{CMB}} = 1089$, and the comoving sound horizon at recombination [53, 54]

$$r_s(z_{\text{CMB}}) = \int_0^{z_{\text{CMB}}} \frac{c_s dt}{a} = cH_0 \int_{z_{\text{CMB}}}^1 \frac{dz}{E(z)} \frac{c_s}{a}; \quad (3)$$

where a is the cosmic scale factor, $a_{\text{CMB}} = 1/(1+z_{\text{CMB}})$, and $a^4 E^2(z) = \frac{m}{m} (a + a_{\text{eq}}) + \frac{k}{k} a^2 + \frac{x}{x} X(z) a^4$, with $a_{\text{eq}} = \frac{rad}{rad} = \frac{m}{m} = 1/(1+z_{\text{eq}})$, and $z_{\text{eq}} = 2.5 \cdot 10^4 \frac{m}{m} h^2 (T_{\text{CMB}} = 2.7 \text{ K})^4$. The sound speed is $c_s = 1 = 3(1 + \frac{R_b}{R_b} a)$, with $\frac{R_b}{R_b} a = 3 \cdot 10^{-4}$, $R_b = 31500 \frac{b h^2}{b} (T_{\text{CMB}} = 2.7 \text{ K})^4$. COBE four year data give $T_{\text{CMB}} = 2.728 \text{ K}$ [52]. The angular scale of the sound horizon at recombination is defined as $l_a = r(z_{\text{CMB}}) = r_s(z_{\text{CMB}})$ [54].

Note that it is important to use the full expression given in Eq.(3) in making predictions for l_a for dynamical dark energy models. Fig.1 shows how the dark energy density $X(z) = x(0)$ compares with the matter density $m(z) = m(0) = (1+z)^3$ for a two parameter dark energy model with dark energy equation of state $w_X(z) = w_0 + w_a(1-a)$ [62] which corresponds to $X(z) = a^{3(1+w_0+w_a)} e^{3w_a(a-1)}$. For models with $w_0 + w_a > 0$, the dark energy contribution to the expansion rate of the universe dominates over that of matter at high z . For models that allow significant early dark energy (as in the $w_X(z) = w_0 + w_a(1-a)$ model), l_a can be underestimated by 20–40% if the dark energy contribution to $r_s(z_{\text{CMB}})$ is ignored.¹

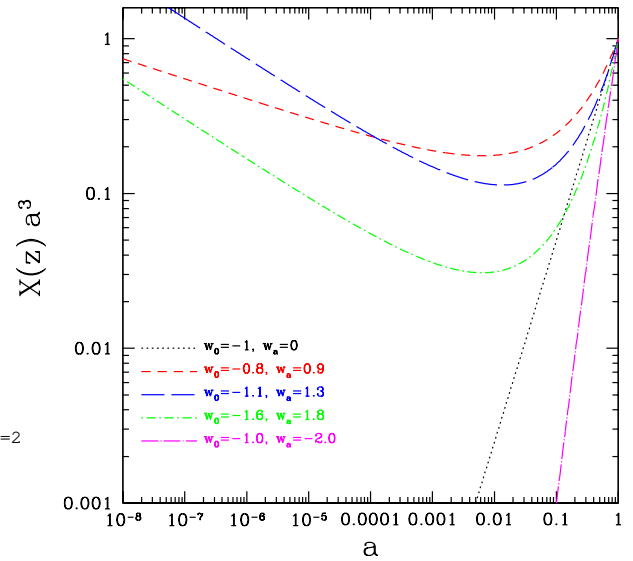


FIG. 1: Ratio of the dark energy density $X(z) = x(0)$ and the matter density $m(z) = m(0) = (1+z)^3$ for dark energy models with dark energy equation of state $w_X(z) = w_0 + w_a(1-a)$.

We will present a consistent and simple framework for using constraints from the CMB data, and give results for using the three-year WMAP observations [55] in the next section.

SN Ia data give the luminosity distance as a function of redshift, $d_L(z) = (1+z)r(z)$. We use 182 SNe Ia from the HST/GOODS program [56] and the first year SNeLS [59], together with nearby SN Ia data, as compiled by [56]. We do not include the ESSENCE data [57], as these are not yet derived using the same method as those used in [56]. Combining SN Ia data derived using different analysis techniques leads to systematic effects in the estimated SN distance moduli [57, 58].

We also use the SDSS baryon acoustic oscillation (BAO) scale measurement [60]. $A = 0.469 (n_s = 0.98)^{0.35} / 0.017$ (independent of a dark energy model) at $z_{\text{BAO}} = 0.35$, where A is defined as

$$A = r^2(z_{\text{BAO}}) \frac{cz_{\text{BAO}}}{H(z_{\text{BAO}})} \frac{1/3}{\frac{m}{m} H_0^{2/3}}: \quad (4)$$

We take the scalar spectral index $n_s = 0.95$ as measured by WMAP 3 [55].²

We run a Monte Carlo Markov Chain (MCMC) based on the MCMC engine of [61] to obtain 10^6 samples

¹ The importance of including the dark energy contribution to l_a is also pointed out by [50].

² Note that the [60] constraint on A depends on the scalar spectral index n_s . Since the error on n_s from WMAP data does not increase the effective error on A , and the correlation of n_s with R and l_a is weak, we have ignored the very weak correlation of A with R and l_a in our likelihood analysis. We have derived R and l_a from WMAP data marginalized over all relevant parameters.

for each set of results presented in this paper. The chains are subsequently appropriately thinned.

We derive constraints on the dark energy density function $X(z) = x(z=0)$ as a free function at $z = z_{\text{cut}}$, with its value at redshifts $z_i = z_{\text{cut}} (i=1, 2, \dots, n)$, $X(z_i)$, treated as n independent parameters estimated from data. We use cubic spline interpolation to obtain values of $X(z)$ at other values of z at $z < z_{\text{cut}}$ [24]. The number of observed SNe Ia is very few beyond z_{cut} . For the currently published SNe Ia, $z_{\text{cut}} = 1.4$. For $z > z_{\text{cut}}$, we assume $X(z)$ to be matched on to either a powerlaw [24]:

$$X(z) = X(z_{\text{cut}}) \frac{1+z}{1+z_{\text{cut}}} ; \quad (5)$$

or an exponential function:

$$X(z) = X(z_{\text{cut}}) e^{(z-z_{\text{cut}})} ; \quad (6)$$

We impose a prior of 3 as z is not bounded from below. Our approach effectively decouples late time dark energy (which is responsible for the observed recent cosmic acceleration and is probed directly by SN Ia data) and early time dark energy (which is poorly constrained) by parameterizing the latter with an additional parameter estimated from data.

For comparison with the results of others, we also derive constraints for models with dark energy equation of state $w_X(z) = w_0 + w_a(1-a)$. This parameterization has the advantage of not requiring a cutto to obtain a finite dark energy equation of state at high z (which is not true for the $w_X(z) = w_0 + w^0 z$ parameterization), but it does allow significant early dark energy (which can cause problems for Big Bang Nucleosynthesis [78] and cosmic structure formation [79]), unless a cutto is imposed. This dilemma illustrates the limited usefulness of simple parameterizations of dark energy.

For all the dark energy constraints presented in this paper, we marginalize the SN Ia data over H_0 in χ^2 -averaging statistics (described in the next subsection), and impose a prior of $H_0 = 72 \pm 8 \text{ (km/s)Mpc}^{-1}$ from the HST Cepheid variable star observations [63].

B. Marginalization over H_0 in SN Ia χ^2 statistics

Because of calibration uncertainties, SN Ia data need to be marginalized over H_0 if SN Ia data are combined with data that are sensitive to the value of H_0 . This is the case here (see the next section). We use the angular scale of the sound horizon at recombination l_a which depends on h^2 , while the dimensionless Hubble parameter $E(z) = H(z)/H_0$ (which appears in the derivation of all distance-redshift relations) depends on m . Hence a dependence on H_0 is implied. We marginalize the SN Ia data over H_0 while imposing a prior of $H_0 = 72 \pm 8 \text{ (km/s)Mpc}^{-1}$ from HST Cepheid variable star observations [63].

The marginalization of SN Ia data over H_0 was derived in [68] for the usual magnitude statistics (assuming that the intrinsic dispersion in SN Ia peak brightness is Gaussian in magnitudes). Here we present the formalism for marginalizing SN Ia data over H_0 in the χ^2 -averaging of SN Ia data using χ^2 statistics (see Eq. [7]). The public software for implementing SN Ia χ^2 averaging with marginalization over H_0 (compatible with cosmoml) is available at <http://www.nhn.ou.edu/~wang/SNcode/>.

Flux-averaging of SN Ia data [58] is needed to minimize the systematic effect of weak lensing of SNe Ia [70]. [66] presented a consistent framework for flux-averaging SN Ia data using χ^2 statistics. If the intrinsic dispersion in SN Ia peak brightness is Gaussian in flux, then³

$$\chi^2_{\text{data}}(s) = \frac{X}{i} \frac{\overline{F}(z_i) - F^p(z_i; s)}{\sqrt{\overline{F}(z_i)}} ; \quad (7)$$

Since the peak brightness of SNe Ia have been given in magnitudes with symmetric error bars, m_{peak} , we obtain equivalent errors in flux:

$$F = \frac{F(m_{\text{peak}} + m) - F(m_{\text{peak}} - m)}{2} ;$$

After χ^2 -averaging, we have

$$\chi^2 = \frac{X}{i} \frac{\overline{F}(z_i) - F^p(\overline{z}_i; s)}{\sqrt{\overline{F}(z_i)}} ; \quad (8)$$

where $F^p(\overline{z}_i; s) = (d_L(\overline{z}_i; s) = M \text{ pc})^2$.

The predicted SN Ia flux $F^p(z_i; s) = d_L(z_i; s) = M \text{ pc}^2 / h^2$. Assuming that the dimensionless Hubble parameter h is uniformly distributed in the range $[0, 1]$, it is straightforward to integrate over h in the probability distribution function to obtain

$$p(s) = h^{-1} = e^{-\chi^2/2} = \frac{\int_0^1 dx e^{-\chi^2(x)}}{\int_0^1 dx e^{-\chi^2(x)}} \quad (9)$$

where

$$\begin{aligned} \chi^2(x) &= \frac{X}{i} \frac{\overline{F}(z_i) - x^2 F^p(\overline{z}_i; s)}{\sqrt{2 \frac{\overline{F}(z_i)}{F(z_i)}}} ; \\ \chi^2_0(x) &= (x^2 - 1)^2 \frac{X}{i} \frac{\overline{F}(z_i)^2}{\sqrt{2 \frac{\overline{F}(z_i)}{F(z_i)}}} ; \end{aligned} \quad (10)$$

where $F^p(\overline{z}_i; s) = F^p(\overline{z}_i; s; h = 1)$.

³ Normally distributed measurement errors are required if the parameter estimate is to be a maximum likelihood estimator [71].

III. RESULTS

A. A Simple and Consistent Framework for Incorporating CMB data

1. Parameter Constraints from CMB data

We have performed MCMC calculations using the full CMB temperature angular power spectrum from WMAP three year observations, without assuming spatial flatness. These calculations are quite time consuming. We have used these to derived the results in Figs.2-3 and Tables I-II.⁴

Fig.2 shows that independent of the assumption about cosmic curvature and dark energy, the three-year WMAP observations give $\omega_m h^2 = 0.12840 \pm 0.0086$, the sound horizon at recombination $r_s(z_{\text{CMB}}) = 148.55 \pm 2.60$ Mpc, and a distance to the recombination surface of $r(z_{\text{CMB}}) = 14305 \pm 285$ Mpc. Note that CMB data do not constrain H_0 in models with nonzero curvature due to parameter degeneracies. For example, the dimensionless Hubble constant $h = 0.50 \pm 0.14$ for a CDM model with $\kappa \neq 0$. It is the absolute scales of $r_s(z_{\text{CMB}})$ and $r(z_{\text{CMB}})$ that are well determined by the CMB data.

Fig.3 shows that allowing nonzero cosmic curvature, the three-year WMAP data give a scaled distance to recombination $R_m H_0^2 r(z_{\text{CMB}}) = 1.71 \pm 0.03$, an angular acoustic scale $l_a r(z_{\text{CMB}}) = r_s(z_{\text{CMB}}) = 302.5 \pm 1.2$, and $bh^2 = 0.02173 \pm 0.00082$, independent of the dark energy model. The corresponding bounds for a flat universe are $R = 1.70 \pm 0.03$, $l_a = 302.2 \pm 1.2$, and $bh^2 = 0.022 \pm 0.00082$. The measured values of (R, l_a, bh^2) differ slightly in a flat universe because of the correlation of curvature with other cosmological parameters when spatial flatness is not assumed.

Table 1 gives the parameters for the Gaussian fits to the probability distribution functions of $(R; l_a; bh^2; \omega_m h^2; r_s(z_{\text{CMB}}); r(z_{\text{CMB}}))$ from the three-year WMAP data. These fits are independent of the dark energy model assumed. Table 2 gives the normalized covariance matrices for $(R; l_a; bh^2; \omega_m h^2; r_s(z_{\text{CMB}}); r(z_{\text{CMB}}))$ from the three-year WMAP data for a CDM model for models with and without curvature. These are appropriate to use with Table 1; models with non-constant dark energy density give slightly smaller correlations between the parameters.

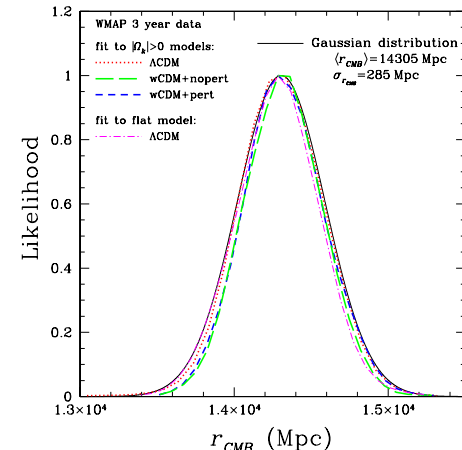
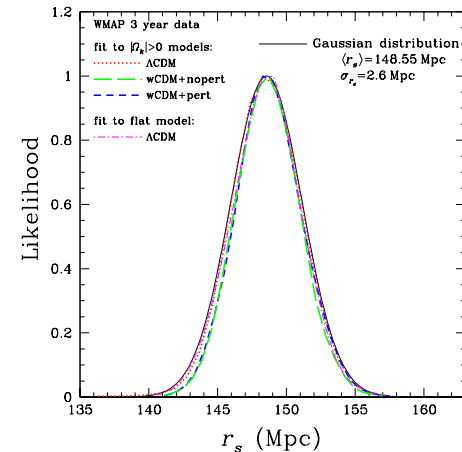
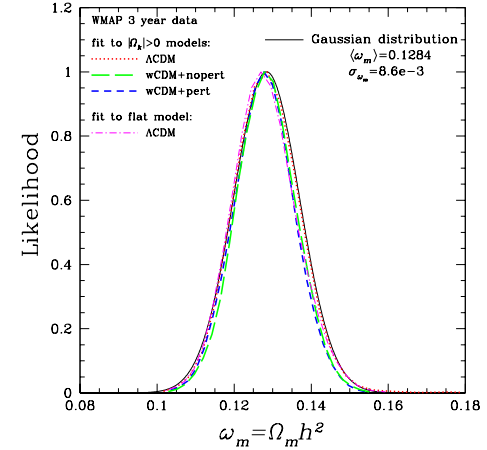


FIG. 2: The matter density $\omega_m h^2$, the sound horizon at recombination $r_s(z_{\text{CMB}})$, and the distance to the recombination surface $r(z_{\text{CMB}})$ from the three-year WMAP data.

⁴ R and l_a are shifted slightly if the running of n_s or/and a nonzero tensor to scalar ratio are considered, and shifted more notably if a nonzero neutrino mass is considered [72]. Current CMB data do not require these additional parameters [55].

TABLE I: The parameters for the Gaussian fits to the probability distribution functions of $(R; l_a; b h^2; m h^2; r_s(z_{CMB}); r(z_{CMB}))$ from the three-year WMAP data, independent of the dark energy model assumed.

Parameter	mean	mean variance
$m h^2$	0.1284	0.0086
$r_s(z_{CMB})/Mpc$	148.55	2.60
$r(z_{CMB})/Mpc$	14305	285
<hr/>		
$k \neq 0$		
R	1.71	0.03
l_a	302.5	1.2
$b h^2$	0.02173	0.00082
<hr/>		
$k = 0$		
R	1.70	0.03
l_a	302.2	1.2
$b h^2$	0.022	0.00082

TABLE II: Normalized covariance matrices for $(R; l_a; b h^2; m h^2; r_s(z_{CMB}); r(z_{CMB}))$ from the WMAP three year.

	R	l_a	$b h^2$	$m h^2$	$r_s(z_{CMB})$	$r(z_{CMB})$
$k \neq 0$						
R	0.1000E+01	0.1237E+00	0.6627E-01	0.9332E+00	0.8805E+00	0.8023E+00
l_a	0.1237E+00	0.1000E+01	0.6722E+00	0.4458E+00	0.5214E+00	0.6569E+00
$b h^2$	0.6627E-01	0.6722E+00	0.1000E+01	0.3731E+00	0.5047E+00	0.5778E+00
$m h^2$	0.9332E+00	0.4458E+00	0.3731E+00	0.1000E+01	0.9882E+00	0.9605E+00
$r_s(z_{CMB})$	0.8805E+00	0.5214E+00	0.5047E+00	0.9882E+00	0.1000E+01	0.9859E+00
$r(z_{CMB})$	0.8023E+00	0.6569E+00	0.5778E+00	0.9605E+00	0.9859E+00	0.1000E+01
$k = 0$						
R	0.1000E+01	0.9047E-01	0.1970E-01	0.9397E+00	0.8864E+00	0.8096E+00
l_a	0.9047E-01	0.1000E+01	0.6283E+00	0.3992E+00	0.4763E+00	0.6185E+00
$b h^2$	0.1970E-01	0.6283E+00	0.1000E+01	0.2741E+00	0.4173E+00	0.4942E+00
$m h^2$	0.9397E+00	0.3992E+00	0.2741E+00	0.1000E+01	0.9876E+00	0.9594E+00
$r_s(z_{CMB})$	0.8864E+00	0.4763E+00	0.4173E+00	0.9876E+00	0.1000E+01	0.9855E+00
$r(z_{CMB})$	0.8096E+00	0.6185E+00	0.4942E+00	0.9594E+00	0.9855E+00	0.1000E+01

2. Two CMB Shift Parameters: R and l_a

Note that although $(m h^2, r_s(z_{CMB}), r(z_{CMB}))$ are tightly constrained by CMB data, they are strongly correlated with each other (see Table 2), hence are not suitable for use in constraining dark energy models. This high degree of correlation arises from how these three parameters are measured. The sound horizon at recombination $r_s(z_{CMB})$ is derived primarily using the measurements of $b h^2$ and $m h^2$ [54], hence is strongly correlated with $m h^2$. The distance to the recombination surface $r(z_{CMB})$ is derived using $r_s(z_{CMB})$ and the angular scale of the sound horizon l_a [54], hence is strongly correlated with $r_s(z_{CMB})$.

Since $r_s(z_{CMB})$ and $r(z_{CMB})$ have different depend-

ences on dark energy and curvature (see Eqs.(1)–(3)), it would be optimal to retain this sensitivity to dark energy and curvature from these two parameters. We find that the scaled distance to recombination, $R = H_0^2 r(z_{CMB})$, and the angular scale of the sound horizon at recombination, $l_a = r(z_{CMB})/r_s(z_{CMB})$, are the scaled parameters (together with $b h^2$) optimal for use in constraining dark energy models, as they retain the sensitivity to dark energy and curvature of $r(z_{CMB})$ and $r_s(z_{CMB})$, and their measured values are nearly uncorrelated (see Table II).

Fig. 4 illustrates the relationship of R and l_a in determining the CMB angular power spectra for simple models that give the same R or l_a values. Fig. 4(a) shows that models that correspond to the same value of R but differ

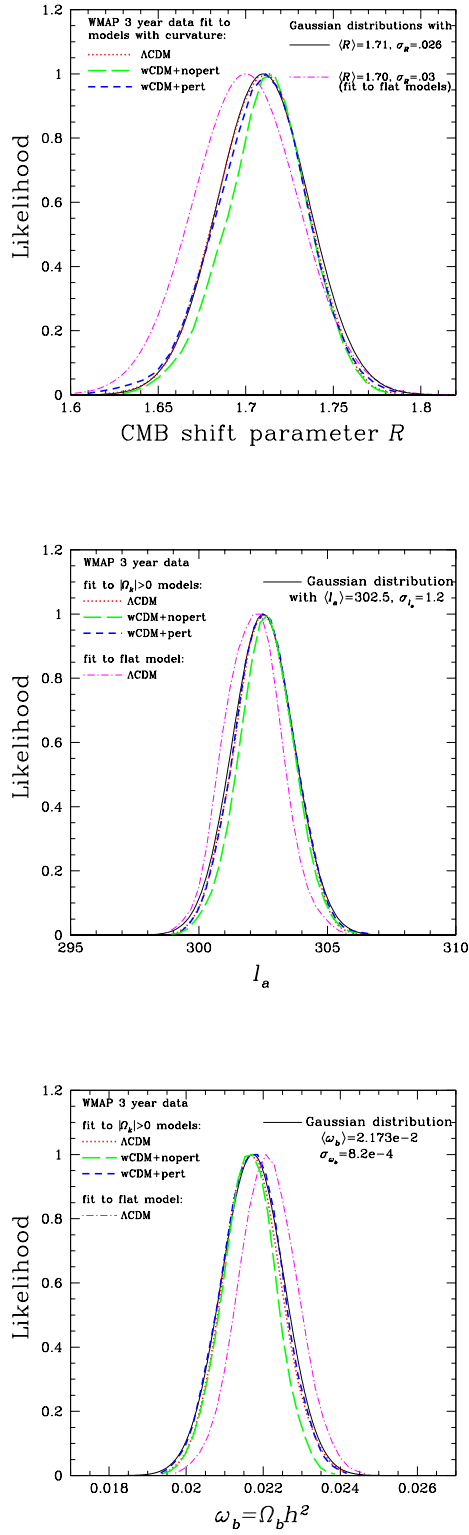


FIG. 3: The scaled distance to recombination R , the angular scale of the sound horizon at recombination l_a , and the baryon density $\Omega_b h^2$ from the three-year WMAP data.

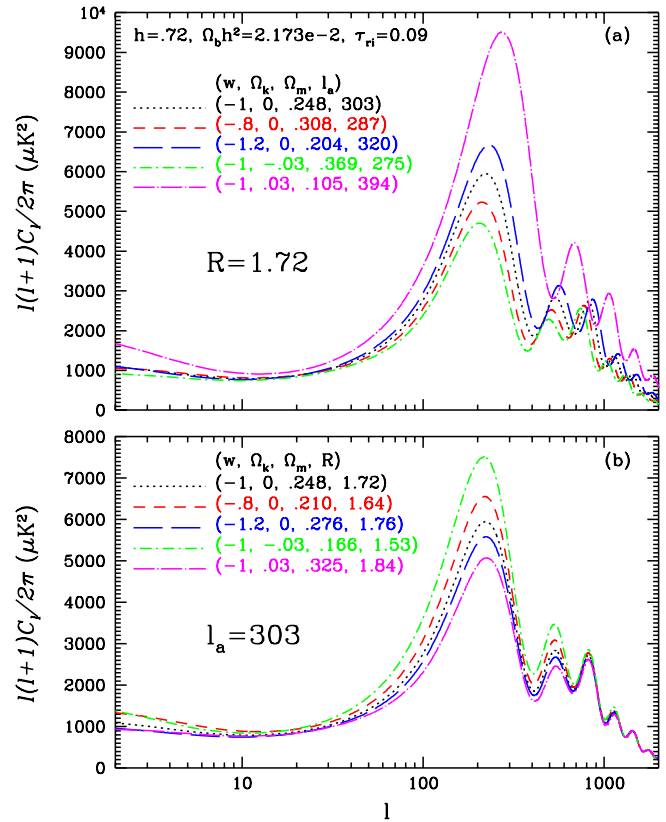


FIG. 4: CMB angular power spectra for dark energy models that give the same values of R or l_a .

ent values of l_a give rise to very different CMB angular power spectra because l_a determines the acoustic peak structure. Fig.4 (b) shows that models that correspond to the same value of l_a but different values of R have the same acoustic peak structure in their CMB angular power spectra, but the overall amplitude of the acoustic peaks is different in each model because of the difference in R .⁵ Clearly, both R and l_a are needed to characterize the CMB angular power spectrum for a given model. R has been known as the CMB shift parameter in the past [64, 65, 66, 67]. [64] showed that in an open universe with a cosmological constant, there is a degeneracy along the $R = 0$ lines, i.e., models with different values of Ω_m , Ω_b , and h that give the same value of R are not distinguishable except at very low multiples (where cosmic variance dominates), see Fig.1 of their paper. Fig.4 here clearly shows that there are two CMB shift parameters, R and l_a , both must be used to describe the complex degeneracies amongst the cosmological parameters that determine the CMB angular power spectrum.

⁵ R is proportional to $\Omega_m h^2$, which determines the overall height of the acoustic peaks.

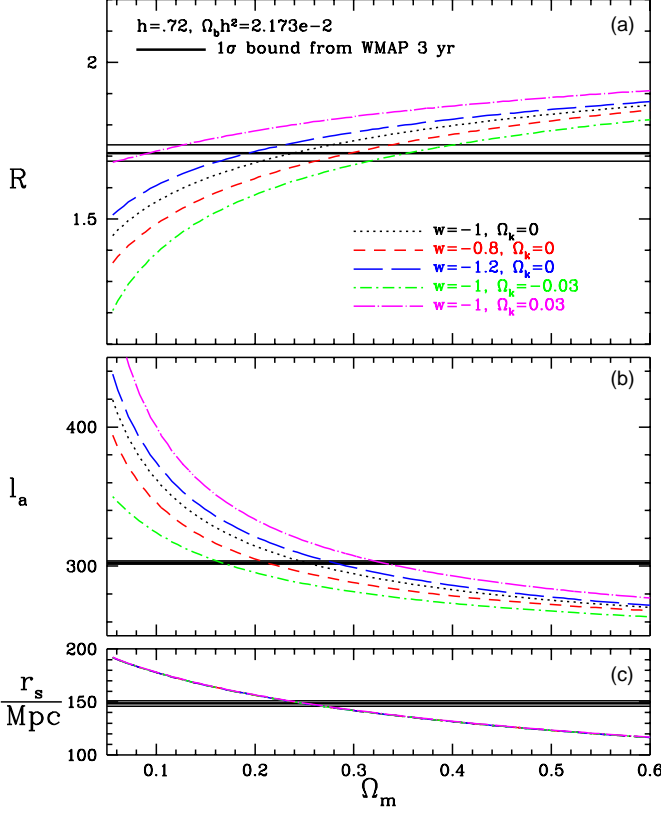


FIG. 5: The expected R and l_a as functions of curvature for five simple dark energy models (with the same line types as in Fig.4).

Now we illustrate how using both R and l_a helps constrain models with a constant dark energy equation of state, and zero or small curvature (the class of models shown in Fig.4). Fig.5 shows the expected R , l_a and $r_s(z_{\text{CMB}})$ as functions of Ω_m for five models. For reference, the values for h and bh^2 have been chosen such that the cosmological constant model satisfies both the R and l_a constraints from WMAP three year data at the same value of Ω_m (as in Fig.4). Note that for the other four models, the R and l_a constraints cannot be satisfied at the same Ω_m value. This is because R and $r_s(z_{\text{CMB}})$ have different dependences on Ω_m . Models that give the wrong R and $r_s(z_{\text{CMB}})$ values can give the right value for l_a because $l_a / R = r_s(z_{\text{CMB}})$. Using both R and l_a constraints thus helps tighten the constraint on Ω_m , which leads to tightened constraints on w or Ω_k .

When more complicated dark energy models and nonzero cosmological curvature are considered, there is a degeneracy between dark energy density function $X(z)$ and curvature. The R or l_a constraints from CMB can always be satisfied with a suitable choice of curvature, but satisfying the R and the l_a constraints usually require different values for curvature. Thus using both R and l_a constraints from CMB helps break the degeneracy between dark energy parameters and curvature. Fig.6

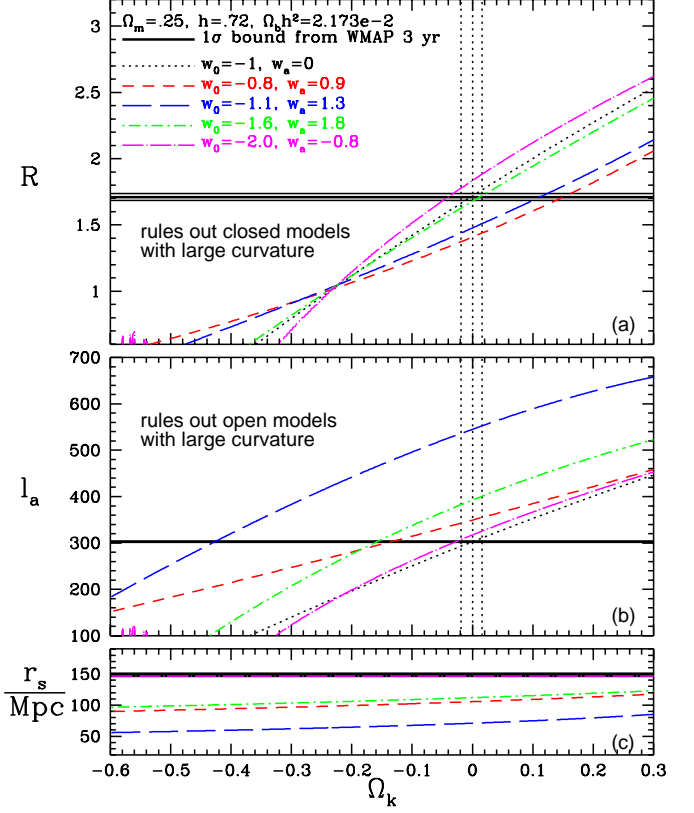


FIG. 6: The expected R and l_a as functions of curvature for the dark energy models from Fig.1 (with the same line types). Both R and l_a are needed to constrain cosmological curvature.

demonstrates this by showing the expected R , l_a , and $r_s(z_{\text{CMB}})$ as functions of curvature for the dark energy models from Fig.1 (with the same line types). For reference, the values for h and bh^2 have been chosen such that the cosmological constant model satisfies both the R and l_a constraints from WMAP three year data. Clearly, the R constraint rules out closed models with large curvature, while the l_a constraint rules out open models with large curvature. The vertical dotted lines indicate the 1-sigma range of Ω_k from R , l_a , and bh^2 constraints from WMAP three year data, combined with the data of 182 SNe Ia, and the SDSS BAO measurement.

Note that the baryon density bh^2 should be included as an estimated parameter in the data analysis. This is because the value of bh^2 is required in making a prediction for l_a in a given dark energy model (see Eq.3), and it is correlated with l_a (see Table II).

To summarize, we recommend that the covariance matrix of (R, l_a, bh^2) given in Tables I-II be used in the data analysis. To implement this, simply add the following term to the χ^2 of a given model with $p_1 = R$, $p_2 = l_a$, and $p_3 = bh^2$:

$$C_{\text{CMB}}^2 = p_i \text{Cov}^{-1}(p_i; p_j) p_j; \quad p_i = p_i - \bar{p}_i^{\text{data}}; \quad (11)$$

where p_i^{data} and the covariance matrix $\text{Cov}(p_i; p_j)$ are given in Tables I-II.

B. Constraints on dark energy

Because of our ignorance of the nature of dark energy, it is important to make model-independent constraints by measuring the dark energy density $\rho_X(z)$ as a free function. Measuring $\rho_X(z)$ has advantages over measuring dark energy equation of state $w_X(z)$ as a free function; $\rho_X(z)$ is more closely related to observables, hence is more tightly constrained [68, 69]. More importantly, measuring $w_X(z)$ implicitly assumes that $\rho_X(z)$ does not change sign in cosmic time (as $\rho_X(z)$ is given by the exponential of an integral over $1 + w_X(z)$); this precludes whole classes of dark energy models in which $\rho_X(z)$ becomes negative in the future ("Big Crunch" models, see [80] for an example) [24].

We have reconstructed the dark energy density function $X(z) = \rho_X(z)/\rho_X(0)$ by measuring its value at $z_i = z_{\text{cut}}(i=3)$ ($i=1, 2, 3$) at $z > z_{\text{cut}}$, and parameterized it by either a powerlaw ($X(z) / (1+z)$) or an exponential function ($X(z) / e^z$) at $z > z_{\text{cut}}$ (see Eqs.(5)–(6)). We have chosen $z_{\text{cut}} = 1.4$ as few SNe Ia have been observed beyond this redshift. We find that current data allow > 0 for $X(z) / (1+z)$ at $z > z_{\text{cut}}$, and require < 0 for $X(z) / e^z$ at $z > z_{\text{cut}}$. This means that assuming powerlaw dark energy at early times allows significant amount of dark energy at $z > 1$, while assuming exponential dark energy at early times is equivalent to postulating dark energy that disappears at $z > 1$. The latter is more physically sensible since dark energy is introduced to explain late time cosmic acceleration. Introducing dark energy that is important at early times could cause problems with Big Bang Nucleosynthesis [78] and formation of cosmic large scale structure [79].

Fig.7 shows the reconstructed dark energy density function $X(z)$ using R , l_a , and bh^2 from the three-year WMAP data, together with 182 SNe Ia and SDSS BAO measurement. Fig.8 shows the corresponding constraints on the cosmic expansion history $H(z)$.

For a flat universe, the dark energy constraints at $z > 1$ are nearly independent of the early time assumption about dark energy, while the dark energy constraint at $z > z_{\text{cut}}$ is more stringent if $X(z) / (1+z)$ at $z > z_{\text{cut}}$. This is as expected. Because of parameter correlations, stronger assumption about early time dark energy (the powerlaw form) leads to more stringent dark energy constraint at late times around $z > z_{\text{cut}}$.

Without assuming a flat universe, in the $X(z) / (1+z)$ at $z > z_{\text{cut}}$ case, there is a strong degeneracy between curvature and the powerlaw index α . This is as expected since the curvature contribution to the total matter-energy density is also a powerlaw, $(1+z)^2$. $X(z)$ is not well constrained in this case, and is not shown in Fig.7. When $X(z) / e^z$ is assumed at $z > z_{\text{cut}}$, there is no degeneracy between the exponential index α and cur-

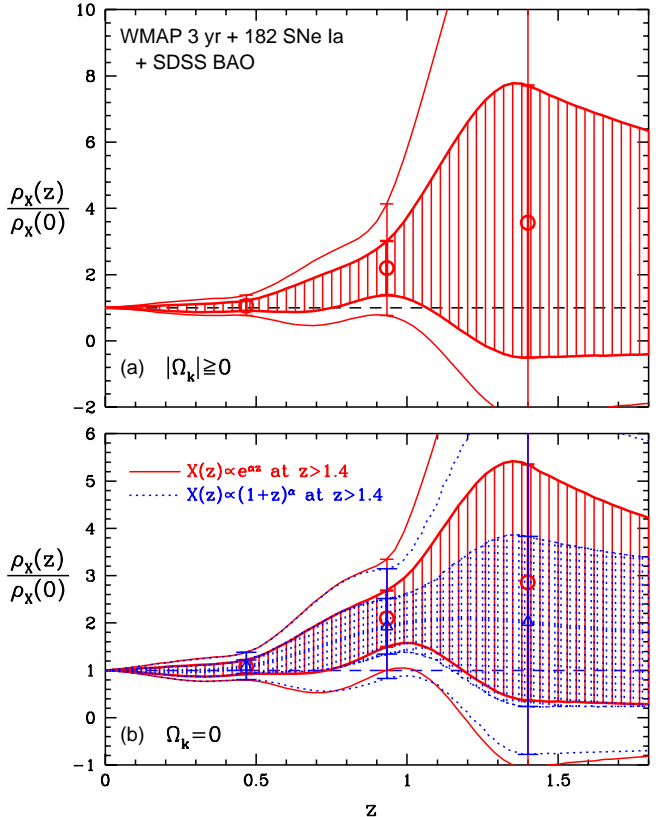


FIG. 7: Constraints on dark energy density using R , l_a , and bh^2 from the three-year WMAP data, together with 182 SNe Ia and SDSS BAO measurement.

vature. $X(z)$ is well constrained in this case (see Fig.7).

For comparison with the work by others, Fig.9 shows the constraints on (w_0, w_a) for models with dark energy equation of state $w_X(z) = w_0 + w_a(1 - a)$, using R , l_a , and bh^2 from the three-year WMAP data, together with 182 SNe Ia and SDSS BAO measurement. These are consistent with the results of [50, 51]. Note that using $w_X(z) = w_0 + w_a(1 - a)$ implies extrapolation of dark energy to early times, which leads to artificially strong constraints (compared to model-independent constraints) on dark energy at both early and late times⁶.

Comparing Fig.7–9 with Figs.3–5 of [67] (for the case of assuming $X(z) / (1+z)$ at $z > z_{\text{cut}}$), it is clear that the constraints on dark energy have significantly tightened if a flat universe is assumed.

⁶ This was noted by [56] as well.

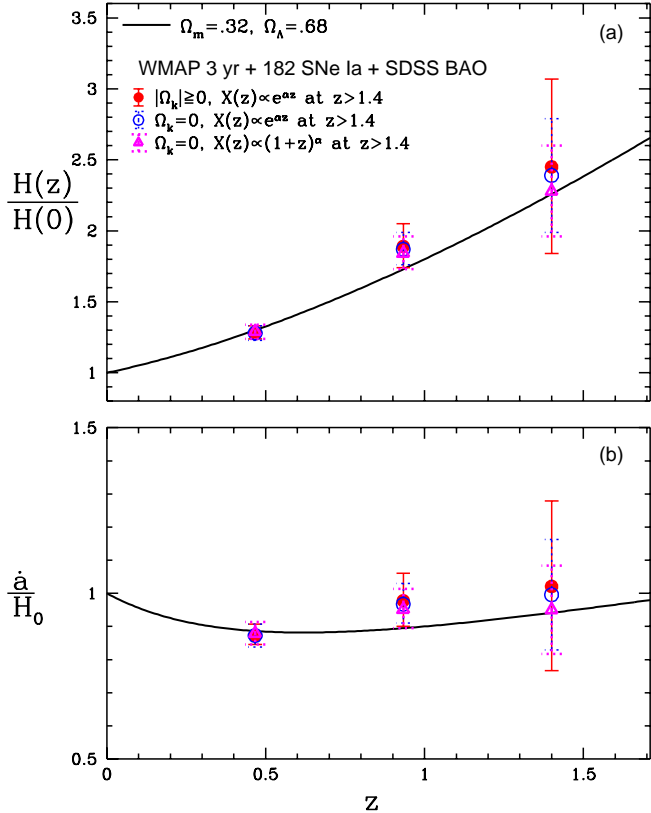


FIG. 8: Constraints on the expansion history of the universe $H(z)$ (Hubble parameter) using R , l_a , and b^2 from the three-year WMAP data, together with 182 SNe Ia and SDSS BAO measurement.

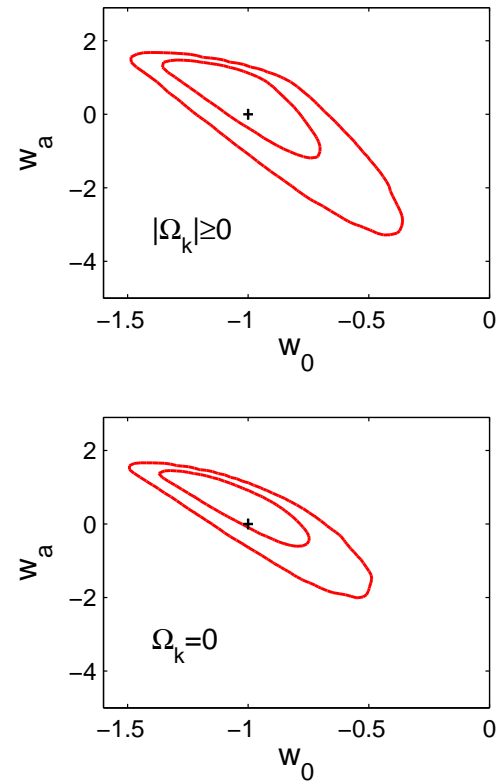


FIG. 9: Constraints on (w_0, w_a) using R , l_a , and b^2 from the three-year WMAP data, together with 182 SNe Ia and SDSS BAO measurement.

C. Cosmological curvature and dark energy constraints

Fig. 10 shows the probability distribution function of cosmological curvature for the model-independent dark energy density $X(z)$ reconstructed in the last subsection, the two parameter dark energy model $w_X(z) = w_0 + w_a(1-a)$, and a constant dark energy equation of state. A universe is allowed at the 68% confidence level in all the cases when curvature is well constrained. Assuming a constant dark energy equation of state gives the most stringent constraints on cosmological curvature. The bounds on cosmological curvature are less stringent if dark energy density is allowed to be a free function of redshift, and are dependent on the assumption about the early time property of dark energy. If dark energy is assumed to be an exponential function at $z > z_{\text{cut}}$ ($z_{\text{cut}} = 1.4$), it is well constrained by current observational data (see Fig. 7) and negligible at early times. In this case, curvature is well constrained as well. If dark energy is assumed to be a power law at early times, its power law index is strongly degenerate with curvature, and neither is well constrained.

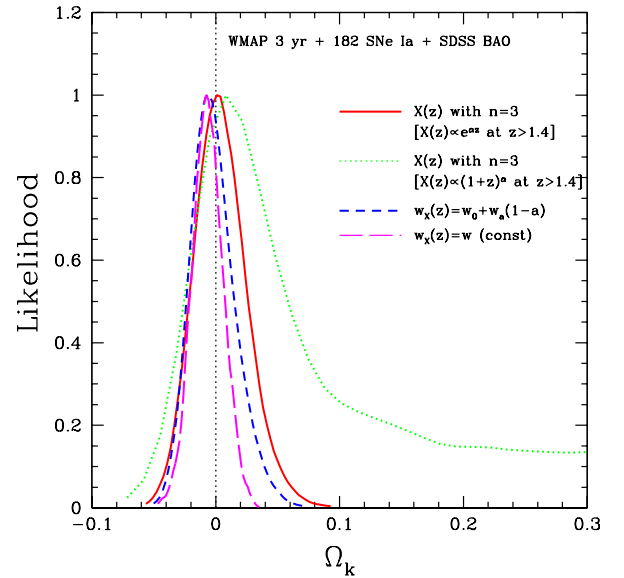


FIG. 10: The probability distribution function of cosmological curvature for the model-independent dark energy density $X(z)$ reconstructed in the last subsection, the two parameter dark energy model $w_X(z) = w_0 + w_a(1-a)$, and a constant dark energy equation of state.

IV. SUMMARY AND DISCUSSION

We have presented a consistent, simple, and effective framework for incorporating constraints from CMB data into an analysis of other cosmological data (for example, SNe Ia and galaxy survey data), when constraining dark energy without assuming a flat universe.

We find that three-year WMAP data give $_{\text{m}} h^2 = 0.1284 \pm 0.0086$, the sound horizon at recombination $r_s(z_{\text{CMB}}) = 148.55 \pm 2.60 \text{ Mpc}$, and a distance to recombination of $r(z_{\text{CMB}}) = 14305 \pm 285 \text{ Mpc}$, independent of the assumption about cosmological curvature and dark energy (see Fig. 2). However, these measurements are strongly correlated and are not suitable for use in constraining dark energy.

We show that there are two CMB shift parameters, $R = \frac{r}{H_0} r(z_{\text{CMB}})$ (the scaled distance to recombination) and $l_a = r(z_{\text{CMB}}) - r_s(z_{\text{CMB}})$ (the angular scale of the sound horizon at recombination); these retain the sensitivity to dark energy and curvature of $r(z_{\text{CMB}})$ and $r_s(z_{\text{CMB}})$, and have measured values that are nearly uncorrelated with each other (see Table II). A allowing nonzero cosmological curvature, the three-year WMAP data give $R = 1.71 \pm 0.03$, $l_a = 302.5 \pm 1.2$, and $_{\text{b}} h^2 = 0.02173 \pm 0.00082$, independent of the dark energy model (see Fig. 3). The corresponding bounds for a flat universe are $R = 1.70 \pm 0.03$, $l_a = 302.2 \pm 1.2$, and $_{\text{b}} h^2 = 0.022 \pm 0.00082$. We give the covariance matrix of $(R, l_a, _{\text{b}} h^2)$ from the WMAP three year data (see Tables I and II).

We demonstrate that both R and l_a (together with $_{\text{b}} h^2$) must be used to describe the complex degeneracies among the cosmological parameters that determine the CMB angular power spectrum (see Fig. 4 and Fig. 5). Using both R and l_a helps break the degeneracy between dark energy density function and cosmological curvature (see Fig. 6).

While completing our paper (based on detailed calculations that have taken several months), we became aware of Ref.[72]. They also found that using both R and l_a tightens dark energy constraints. However, their paper assumed a flat universe, and used an approximation for l_a that ignores both curvature and dark energy contributions. We use the exact expression for l_a and derived the

⁷ Ref[35] studied the statistical consistency of subsets of SNe Ia that comprise the 182 SNe Ia.

covariance matrix for $(R, l_a, _{\text{b}} h^2)$ which are based on the MCMC chains from our full CMB power spectrum calculations without assuming spatial flatness.

We have used R , l_a , and $_{\text{b}} h^2$ from WMAP three year data, together with 182 SNe Ia (from the HST/GOODS program, the first year Supernova Legacy Survey, and nearby SN Ia surveys), and SDSS measurement of the baryon acoustic oscillation scale in deriving constraints on dark energy. Assuming the HST prior of $H_0 = 72 \pm 8 \text{ km/s/Mpc}$ [63], we find that current observational data provide significantly tightened constraints on dark energy models in a flat universe, and less stringent constraints on dark energy without assuming spatial flatness (see Figs. 7-9). Dark energy density is consistent with a constant in cosmological time, with marginal deviations from a cosmological constant that may reflect current systematic uncertainties⁷ or true evolution in dark energy (see Figs. 7-8). Our findings are consistent with that of [56] and [41].

A flat universe is allowed by current data at the 68% confidence level. As expected, the bounds on cosmological curvature are less stringent if dark energy density is allowed to be a free function of cosmological time, and are also dependent on assumption about dark energy properties at early times (see Fig. 10). The behavior of dark energy at late times (where it causes cosmological acceleration and is directly probed by SN Ia data) and at early times (where it is poorly constrained) should be separated in parameter estimation in order to place robust constraints on dark energy and cosmological curvature (see Sec. II B and C).

Future dark energy experiments from both ground and space [73, 74, 75, 76], together with CMB data from Planck [77], will dramatically improve our ability to probe dark energy, and eventually shed light on the nature of dark energy.

Acknowledgments We thank Jan Michael Kratochvil for being a strong advocate of marginalizing SN Ia data over H_0 ; Savas Nesseris, Leandros Perivolaropoulos, and Andrew Liddle for useful discussions. We gratefully acknowledge the use of camb and cosmomc. This work was supported in part by NSF CAREER grants AST-0094335 (YW). PM is funded by PPARC (UK).

- [1] Riess, A. G., et al, 1998, *Astron. J.*, 116, 1009
- [2] Perlmutter, S. et al, 1999, *ApJ*, 517, 565
- [3] Freese, K., Adams, F. C., Frieman, J. A., and Mottola, E., *Nucl. Phys. B* 287, 797 (1987).
- [4] Linde A D, "Inflation And Quantum Cosmology," in *Three hundred years of gravitation*, (Eds.: Hawking, S. W. and Israel, W., Cambridge Univ. Press, 1987), 604-630.
- [5] Peebles, P. J. E., and Ratra, B., 1988, *ApJ*, 325, L17
- [6] Wetterich, C., 1988, *Nucl. Phys. B* 302, 668

- [7] Frieman, J. A., Hill, C. T., Stebbins, A., and Waga, I., 1995, *PRL*, 75, 2077
- [8] Caldwell, R., Dave, R., & Steinhardt, P. J., 1998, *PRL*, 80, 1582
- [9] Sahni, V., & Habib, S., 1998, *PRL*, 81, 1766
- [10] Parker, L., and Raval, A., 1999, *PRD*, 60, 063512
- [11] Boisseau, B., Esposito-Farese, G., Polarski, D., & Starobinsky, A. A. 2000, *Phys. Rev. Lett.*, 85, 2236
- [12] Dvali, G., Gabadadze, G., & Pomarol, M. 2000, *Phys. Lett.*

B 485, 208

[13] M ersini, L., B astero-G il, M ., & K anti, P ., 2001, PRD , 64, 043508

[14] F reese, K ., & Lew is, M ., 2002, Phys. Lett. B , 540, 1

[15] Padmanabhan, T ., 2003, Phys. Rep. , 380, 235

[16] Peebles, P J E ., & Ratra, B ., 2003, Rev. Mod. Phys. , 75, 559

[17] Carroll, S M ., de Felice, A ., D uvvuri, V ., Easson, D A ., Trodden, M . & Turner, M . S., Phys. Rev. D 71 (2005) 063513

[18] O nem li, V . K ., & W oodard, R . P . 2004, Phys. Rev. D 70, 107301

[19] Cardone, V . F ., Tortora, C ., Troisi, A ., & Capozziello, S ., 2005, astro-ph/0511528, Phys. Rev. D , in press

[20] Kolb, E W ., M atarrese, S ., & Riotto, A ., 2005, astro-ph/0506534

[21] Caldwell, R .R .; Kom p, W .; Parker, L .; Vanzella, D A T ., Phys. Rev. D 73 (2006) 023513

[22] Koivisto, T .; M ota, D F ., hep-th/0609155, Phys. Rev. D 75 (2007) 023518

[23] Ng, Y .J ., gr-qc/0703096

[24] W ang, Y ., & Tegmark, M . 2004, Phys. Rev. Lett. , 92, 241302

[25] W ang, Y ., & Tegmark, M . 2005, Phys. Rev. D 71, 103513

[26] Lam, U ., & Sahni, V . 2005, astro-ph/0511473

[27] Daly, R .A . & Djorgovski, S .G . 2005, astro-ph/0512576.

[28] Jassal, H K ., Bagla, J S ., Padmanabhan, T ., 2005, Phys. Rev. D 72, 103503

[29] Jassal, H K ., Bagla, J S ., Padmanabhan, T ., 2005, Mon. Not. R. Astron. Soc. Letters , 356, L11

[30] Barger, V .; Gao, Y .; M arfatia, D ., astro-ph/0611775

[31] Dick, J ., K nox, L ., & Chu, M . 2006, astro-ph/0603247

[32] H uterer, D .; Peiris, H .V ., astro-ph/0610427

[33] Jassal, H K ., Bagla, J S ., Padmanabhan, T ., 2006, astro-ph/0601389

[34] Liddle, A R .; Mukherjee, P .; Parkinson, D .; W ang, Y ., PRD , 74, 123506 (2006), astro-ph/0610126

[35] N esseris, S ., & Perivolaropoulos, L ., 2006, astro-ph/0602053; N esseris, S ., & Perivolaropoulos, L ., 2006, astro-ph/0612653

[36] Schmid, C . et al. 2006, astro-ph/0603158

[37] Samushia, L .; Ratra, B ., A strophys. J. 650 (2006) L5

[38] Wilson, K M ., Chen, G ., Ratra, B ., 2006, astro-ph/0602321

[39] Xia, J.-Q .; Zhao, G .B .; Li, H .; Feng, B .; Zhang, X ., Phys. Rev. D 74 (2006) 083521

[40] Lam, U .; Sahni, V .; Starobinsky, A A ., astro-ph/0612381, JCAP 0702 (2007) 011

[41] Davis, T .M ., et al. 2007, astro-ph/0701510

[42] Wei, H .; Zhang, S N ., astro-ph/0609597, Phys. Lett. B 644 (2007) 7

[43] Zhang, J .; Zhang, X .; Liu, H ., astro-ph/0612642

[44] Zundel, C .; Trotta, R ., astro-ph/0702695

[45] Tegmark, M ., et al. 2004, ApJ, 606, 702

[46] Verde, L ., et al. 2002, MNRAS , 335, 432; Hawkins, E ., et al. 2003, MNRAS , 346, 78

[47] Clarkson, C .; Cortes, M .; Bassett, B A ., astro-ph/0702670

[48] Gong, Y .; W ang, A ., astro-ph/0612196, Phys. Rev. D 75 (2007) 043520

[49] Ichikawa, K .; Takahashi, T ., astro-ph/0612739, JCAP 0702 (2007) 001

[50] Wright, E L ., astro-ph/0701584

[51] Zhao, G ., et al., astro-ph/0612728

[52] Fixsen, D .J ., 1996, ApJ, 473, 576

[53] Eisenstein, D . & Hu, W . 1998, ApJ, 496, 605

[54] Page, L ., et al. 2003, ApJS , 148, 233

[55] Spergel, D N ., et al. 2006, astro-ph/0603449, ApJ, in press

[56] Riess, A G ., et al., astro-ph/0611572

[57] Wood-Vasey, W . M ., et al., astro-ph/0701041

[58] W ang, Y ., ApJ 536, 531 (2000)

[59] Astier, P ., et al. 2005, astro-ph/0510447, A stron. A strophys. 447 (2006) 31

[60] Eisenstein, D ., et al., ApJ, 633, 560

[61] Lewis, A ., & Bridle, S . 2002, PRD , 66, 103511

[62] Chevallier, M ., & Polarski, D ., 2001, Int. J. Mod. Phys. D 10, 213

[63] Freedman, W . L ., et al. 2001, ApJ, 553, 47

[64] Bond, J. R ., Efstathiou, G ., & Tegmark, M ., 1997, MNRAS , 291, L33

[65] Odman, C J ., M elchiorri, A ., Hobson, M .P ., & Lasenby, A .N ., 2003, Phys. Rev. D 67, 083511

[66] W ang, Y ., & Mukherjee, P ., 2004, ApJ, 606, 654

[67] W ang, Y ., & Mukherjee, P ., 2006, ApJ, 650, 1

[68] W ang, Y ., and Gamovich, P ., 2001, ApJ, 552, 445

[69] Tegmark, M ., 2002, Phys. Rev. D 66, 103507

[70] Kantowski, R ., Vaughan, T ., & Branch, D ., 1995, ApJ, 447, 35; Frieman, J. A ., 1997, Comments A strophys. , 18, 323; W ambganss, J ., Cen, R ., Xu, G ., & O stricker, J.P ., 1997, ApJ, 475, L81; Holz, D E ., 1998, ApJ, 506, L1; W ang, Y ., 1999, ApJ, 525, 651

[71] Press, W .H ., Teukolsky, S A ., Vettering, W .T ., & Flannery, B P ., 1994, Numerical R ecipes, Cambridge University Press, Cambridge.

[72] Elgaroy, O ., and M ultamaki, T ., astro-ph/0702343.

[73] W ang, Y ., 2000, ApJ 531, 676

[74] Albrecht, A .; Bernstein, G .; Cahn, R .; Freedman, W .L .; Hewitt, J .; Hu, W .; Huth, J .; Kamionkowski, M .; Kolb, E W .; K nox, L .; M ather, J.C .; Staggs, S .; Suntze, N B ., Report of the Dark Energy Task Force, astro-ph/0609591

[75] See for example, <http://www.astro.ubc.ca/LMT/alpaca/>; <http://www.lsst.org/>; <http://www.asutexas.edu/hetdex/>.

[74] contains a more complete list of future dark energy experiments.

[76] W ang, Y ., et al., BAAS , v36, n5, 1560 (2004); Crotts, A ., et al. (2005), astro-ph/0507043; Cheng, E .; W ang, Y ., et al., Proc. of SPIE , Vol. 6265, 626529 (2006); <http://jedinhn.ou.edu/>

[77] Planck Bluebook, http://www.rssd.esa.int/index.php?project=PLA_N

[78] Steigman, G ., 2006, astro-ph/0611209

[79] Sandvik, H .; Tegmark, M .; Zaldarriaga, M .; Waga, I ., 2004, Phys. Rev. D 69 (2004) 123524

[80] W ang, Y .; K ratochvil, J.M .; Linde, A .; Shmakova, M ., 2004, JCAP , 12, 006 (2004), astro-ph/0409264